Materials and Design 195 (2020) 109050

Contents lists available at ScienceDirect

Materials and Design

journal homepage: www.elsevier.com/locate/matdes

Nanofibre toughening of dissimilar interfaces in composites

Timo Meireman, Lode Daelemans, Elisa Van Verre, Wim Van Paepegem, Karen De Clerck *

Department of Materials, Textiles and Chemical Engineering (MaTCh), Ghent University, Technologiepark 70A, Zwijnaarde B-9052, Belgium

HIGHLIGHTS

- For the first time, the delamination resistance of diverse dissimilar interfaces is highly increased by nanofibre toughening.
- An extensive mode I and II increase of respectively 30–50% and 70–130% was achieved for each considered dissimilar interface.
- The crack path repeatedly crosses the nanofibre toughened zone which largely contributes to the increased fracture toughness.
- Crack bifurcations develop towards adjacent interfaces due to the improved toughness of nanotoughened dissimilar interfaces.

GRAPHICAL ABSTRACT

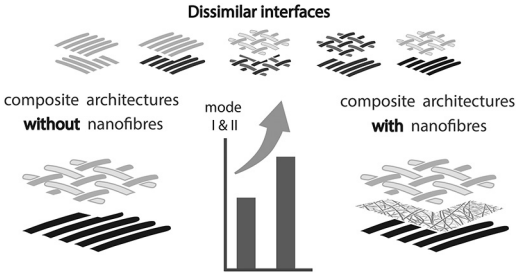

ARTICLE INFO

Article history:
Received 18 May 2020
Received in revised form 1 August 2020
Accepted 6 August 2020
Available online 11 August 2020

Keywords:
Nanocomposites
Matrix cracking
Interface debonding
Nanofibre bridging
Electrospinning
Hybrid composite

ABSTRACT

Fibre reinforced composite laminates are key engineering materials allowing to design lightweight components with high mechanical properties. Yet they are prone to delamination between the reinforcing plies, which in turn limits the damage resistance of many applications. This is especially true for the interfaces between dissimilar reinforcing plies that are often encountered in actual components, e.g. differences in fibre orientation, fibre material or ply architecture, where high interlaminar stresses can occur. Nanofibrous toughening veils are known to increase the damage resistance when inserted between similar reinforcing plies, but it is currently unknown how they perform when delamination occurs at dissimilar interfaces. Here, the nanofibre toughening of frequently encountered dissimilar interfaces such as occurring between multidirectionally stacked unidirectional fibre plies (+45°/−45°), multistructural stackings (unidirectional versus fabrics) and multimaterial configurations (glass fibres versus carbon fibres) are analysed. These interfaces largely exert their influence on the crack path during delamination and thus alter the effectiveness of nanofibre toughening. Poly(ether-*block*-amide) nanofibres of the biosourced polyamide 11 family result in a large increase in mode I and mode II interlaminar fracture toughness for all the tested dissimilar interfaces. We show that their effectiveness however depends on the underlying delamination mechanics present in different dissimilar interfaces.

1. Introduction

Fibre reinforced composite materials are often desired in advanced applications such as in aerospace, wind turbines and sports equipment. These high performance materials are preferred due to their low weight, high stiffness and strength. Depending on the material requirements for

* Corresponding author.
E-mail address: Karen.DeClerck@UGent.be (K. De Clerck).

https://doi.org/10.1016/j.matdes.2020.109050

different applications, the composite material needs a tailor-made design by varying the choice and orientation of consecutive composite plies. It is thus a regular practice to use the advantages of different layers and combine them within the same composite structure [1–8]. For example, in wind turbines and the automotive industry, carbon fibres that provide very high specific strength and stiffness are used together with cheaper glass fibres to cut costs and increase efficiency [3,4,9,10]. It is also common to stack unidirectional (UD) fibre plies in different orientations and combine them with woven layers in order to obtain the desired material stiffness and strength in each direction [2,11–15]. Fig. 1 shows the variety of research that highlights the importance and synergetic effects of composites with dissimilar interfaces in high-end material applications and designs.

Despite their numerous advantages, a major downside of composites is their failure by delamination. This is certainly the case at dissimilar interfaces because the two neighbouring reinforcement layers can have large differences in elastic properties, which create high interlaminar stresses that make these areas even more susceptible to delamination in comparison with similar interfaces [9,10]. The susceptibility of the hybrid interlayer to delamination makes it one of the weakest links in the composite structure and thus toughening the material is recommended for designing high performance applications.

An emerging method for increasing the interlaminar fracture toughness (IFT), is by interleaving thin electrospun nanofibrous veils between the composite laminates [23–28]. The nanofibres can be deposited directly onto the reinforcing plies prior to infusion or autoclaving and thus, they do not influence the viscosity of the resin. Additionally, they have a wide industrial potential as they can be produced from low toxicity polymers, have minimal risk of airborne nanosized particles and the presence of nanofibres has no detrimental effect on the in-plane mechanical tensile and shear properties [29]. A variety of industrial electrospinning machines are already available nowadays that allow commercial usage of nanofibres for toughening of composites with a variety of main reinforcement fibres and resin types [30–32]. A recent review by Zucchelli and Palazzetti provides a great summary of this field of nanofibre toughening showing the wide variety of polymer nanofibre materials that have been used [27]. The toughening effect of the nanofibres is directly dependent on the effects of nanofibre bridging of the crack and yielding of the nanofibres, which has also been shown by Beckermann and Pickering [33]. The fracture behaviour is on its turn influenced by the adhesive interactions between matrix and nanofibre and the properties of the nanofibre material itself [24–29,33–36].

A broad range of nanofibres with various thermomechanical properties have already been investigated in the state of the art for their use as nanofibre tougheners in composites, including polyamides [26,27,34,37], polyacrylonitrile [38], polycaprolactone (PCL) [26,27], polyvinylalcohol [27,39], polyvinyl Butyral [33] and poly(vinylidene fluoride) [38,40]. Based on our previous research and literature, poly (ether-*block*-amide) (PEBA) polymers are one of the best polymers suitable for nanofibre toughening because it is a temperature stable, eco-friendly, commercial viable system that allows for versatile toughening with major improvements in both mode I (+50%) and mode II (+100%) IFT [27,34].

In our previous work, we showed that the crack path of the delamination should frequently pass through the nanofibre-toughened zone in order for the nanofibres being able to exert their toughening effect [29,34,41]. During typical mode I and mode II IFT tests, UD fibres of the same material type (such as carbon or glass fibres) were used, which were all stacked in parallel [23–27].

Yet, the nanofibre toughening of dissimilar interfaces has not been studied to date while the fracture toughness of dissimilar interfaces without any nanofibrous reinforcement has been examined and shown to be different from the similar case [2,13]. For example in the case of multidirectional interfaces the increase of interface angle causes the mode I fracture propagation toughness to increase through a different fracture mechanism that includes more fibre bridging and debonding [2]. Another example is the combination of woven carbon plies on the outer layers of UD carbon laminates. Several researchers

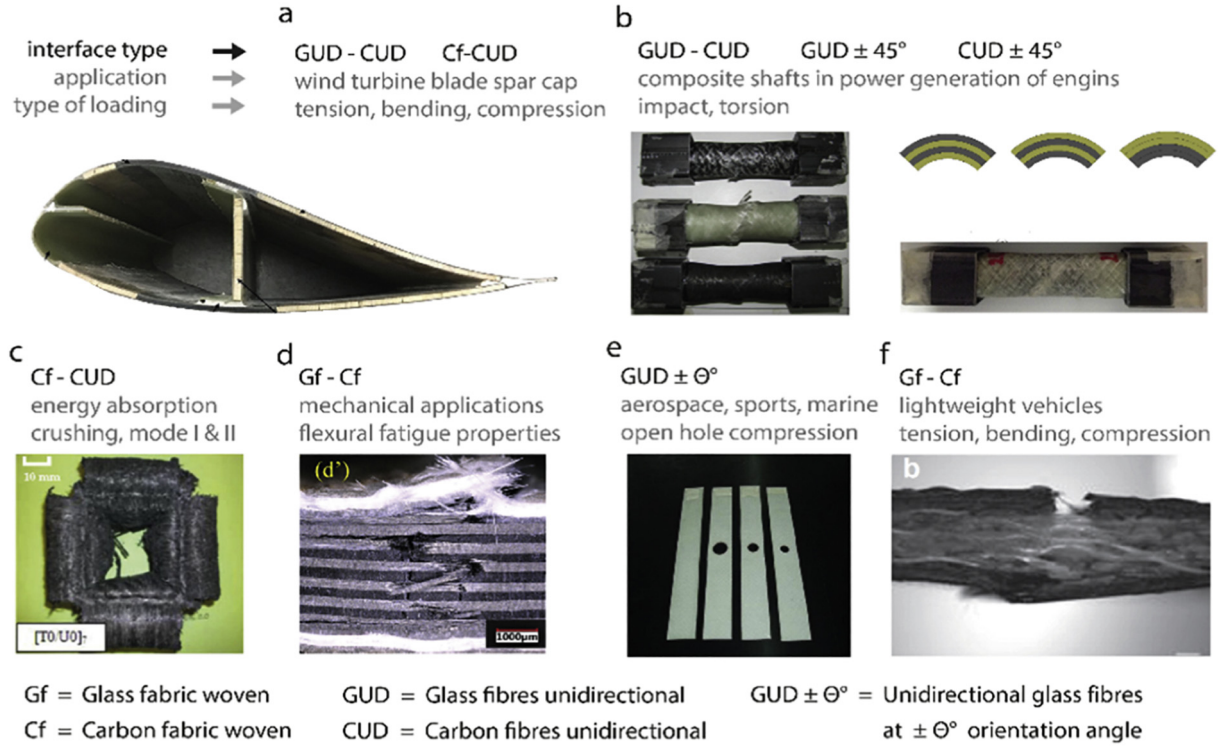

Fig. 1. Research addresses the synergetic effects of dissimilar interfaces in composites that are used in a variety of high-end applications that often require lightweight, high stiffness and strength. Examples are shown of research on multimaterial (a [16], b [17,18], d [19], f [20]), multidirectional (b, e [21]) and multistructural (a, c [22]) composites.

noted a positive influence in impact tests and on the residual strength in Compression After Impact tests [6,7,42] because the woven structure prevents the formation of large intralaminar cracks. The influence of residual thermal stresses will generally have a minimal influence on the competition between interface debonding and further crack penetration in adjacent layers of fibre reinforced composites with dissimilar interfaces [43,44]. The residual stresses mainly influence the load level at which fracture starts but not the mechanism itself [45].

It can thus be expected that the nanofibre toughening will also be affected by the type of dissimilar interface. Because the interaction between the crack path and the toughened interlayer is a key component in successful nanofibre toughening, it is of utmost importance to study the ability of the nanofibres to improve the fracture toughness of these dissimilar interfaces as well. To do so, we focus in this manuscript on the nanofibre toughening of dissimilar interfaces that are split up into three common categories: (i) multidirectional (different orientation of interfaces), (ii) multimaterial (e.g. glass-carbon) and (iii) multistructural (UD-woven) interfaces.

We first discuss the mode I and mode II IFT of composites with dissimilar interfaces in the absence of any nanofibres. Subsequently, composites are produced in which the dissimilar interface is toughened by interleaving electrospun nanofibrous membranes made from PEBA polymer. For each interface type, a microscopic analysis of the fracture surfaces is performed to understand the micromechanical mechanisms of the nanofibre toughening for that specific case, and, to relate it to the toughening efficiency.

2. Materials and methods

2.1. Nanofibre veil preparation

Pebax® Rnew® 72R53 SP 01 resin [referred to as PEBA72 onwards] was kindly received from Arkema. The pellets were dissolved for electrospinning at 8 wt% in a mixture of 60% formic acid and 40% anisole, both purchased from Sigma – Aldrich. Both solvents were used as received. An in-house developed electrospinning machine based on a multinozzle design was used to deposit the nanofibres directly onto glass and carbon fibre plies at 2.5 g/m^2 similar to our previous paper [29]. PEBA was electrospun at 2 ml/h. A 6 cm Tip to Collector Distance was used. A high voltage power supply (Glassman High Voltage Series) was used to apply 30 kV for stable electrospinning. Representative Scanning Electron Microscopy (SEM) images were taken and nanofibre diameters were measured on dry samples prior to resin infusion. The nanofibre diameter of 190 ± 40 nm was measured on at least 50 fibres with the software package ImageJ [46]. More information about the electrospinning can be found in Ref. [34].

2.2. Composite production and testing

Laminates with PEBA72 nanofibres in the interlayer as well as non-toughened reference laminates without nanofibre reinforcements were manufactured by Vacuum Assisted Resin Transfer Molding (VARTM) using four different types of reinforcements which are listed in Table 1.

The nanofibres were directly spun onto the reinforcing plies at the side facing the midplane (delamination plane) and thus totalled an amount of 5 g/m^2 in the interlayer. The epoxy resin (EPIKOTE MGS RIMR135) and hardener (EPIKURE MGS RIMH137) were supplied by Momentive and used in a 100:30 mass ratio. Curing at 80 °C for 5 h (validated by Differential Scanning Calorimetry to complete curing reaction) was initiated immediately after resin impregnation of the composite. A 25 μm thick ethylene tetrafluoroethylene-based release film was inserted at the dissimilar interface to serve as an initial delamination in the mode I and II delamination experiments.

The mode I IFT (G_{IC}) was evaluated by the Double Cantilever Beam (DCB) and the mode II IFT (G_{IC}) was determined by End Notched Flexure (ENF) according to the compliance based beam method such as previously reported [41,47]. A displacement controlled Instron 3369 equipped with a 500 N and 2000 N load cell was used to perform the DCB and the ENF tests, respectively.

Table 1
Fabric properties of the main glass and carbon fibre reinforcements for both UD and woven fabrics.

	Carbon UD	Carbon fabric	Glass UD	Glass fabric
Areal density	400 g/m^2	245 g/m^2	500 g/m^2	390 g/m^2
Weave pattern	Unidirectional	Twill 2 × 2	Unidirectional	Twill 2 × 2
Fibre material	Carbon	Carbon	Glass	Glass
Yarn description				
Warp (tex)		200		340
Weft (tex)		200		272
Thread Count				
Warp (per cm)		6		6
Weft (per cm)		6		6.7
Producer	R&G Faserverbund-werkstoffe GMBH	R&G Faserverbund-werkstoffe GMBH	SGL Group - The Carbon Company	Interglass

The mode I IFT was calculated according to the ASTM D5528 method (Eq. (1)) [48]. Where P is the critical load, δ is the critical displacement, b is the width, a is the delamination length, Δ corrects for crack front rotations and F corrects for large displacement effects of the piano hinges. The G_{IC} was determined from the load-displacement curves at the 5%/max point as described in the ASTM standard. The mode I pre-crack was produced naturally by loading to crack initiation and directly unloading the specimen. The propagation value was determined of the plateau in the R-curve. Delamination tests were performed at a rate of 2 mm/min and the crack was monitored using a traveling microscope.

The mode II IFT GIIc was calculated using the Compliance Based Beam Method (Eq. (2)) as described in previous work [47] with P the maximum load and a_{eq} the equivalent delamination length based on the specimen compliance as described in Reference [29]. E_f is the flexural modulus, b is the width, 2 h is the specimen thickness, and |1 - ζ| corrects for large displacement effects. The initiation was determined at the point of maximum load in the ENF experiment. The initial delamination length of 37.5 mm and span of 100 mm resulted in stable crack growth. The samples were loaded under three point bending at 1 mm/min.

$$G_{IC} = \frac{3P\delta}{2b(a+|\Delta|)}F \tag{1}$$

$$G_{IIC} = \frac{9P^2a_{eq}^2}{2E_f b^2(2h)^3}|1-\zeta| \tag{2}$$

For mode I IFT, both initiation IFT and propagation IFT were determined, while for mode II only the initiation IFT was recorded as it is experimentally rather complex to measure the crack growth accurately under mode II delamination. Representative load-displacement curves are added as supplementary information (S1). At least three samples were tested for each configuration. Multiple SEM images were taken to study the fracture surface of DCB and ENF loaded specimens. Optical microscopy was used to study the crack development of lateral cross-sections of the test samples after being subjected to mode I and mode II tests (Fig. 2).

In order to perform the DCB/ENF tests correctly, the composite samples were designed such that the specimen legs of the samples bend symmetrically during testing. Hence, the bending stiffness (S) of both legs, which differ in layup and/or material and are separated by the

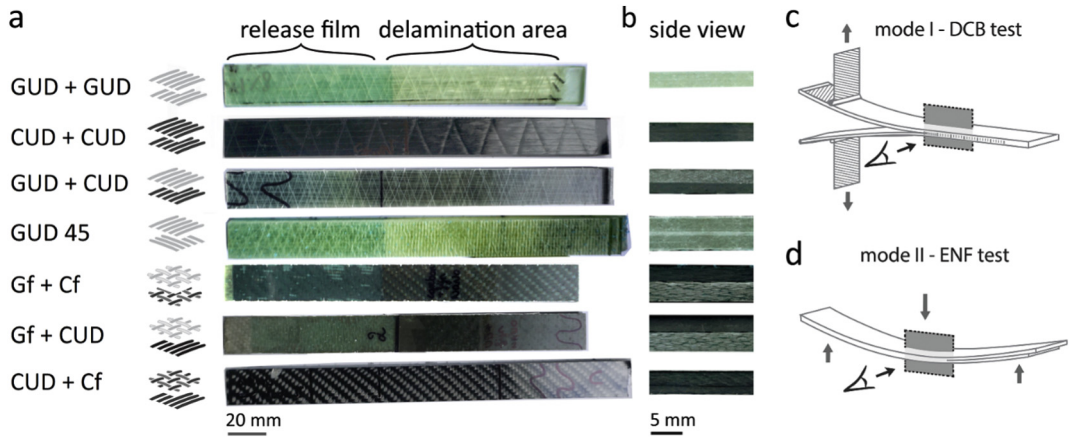

Fig. 2. The different types of tested composite samples (a) with their side view (b). Optical microscopy was used to study the lateral cross-section of both mode I (c) and mode II (d) samples.

release film, needed to be the same. S was calculated for each leg from the flexural modulus (E) and the second moment of area (I_x) of the rectangular test samples (Eq. (3)). For this, E was calculated with the slope of the linear section of the extension-load curve (m) of a three-point bending test with width (b) and thickness (h) of the samples and span length (L = 32 h). The optimal stackings were selected such as shown in Table 2. No significant difference (one-tailed *t*-test, alpha = 0.05) in thickness between the non-toughened and toughened

Table 2
Stacking sequence for each interface evaluated for nanofibre toughening. For the non-symmetric delamination specimens, the bending stiffness of the individual specimen-halves is given. Fabrics were always stacked with the warp yarns in the 0° direction.

Name	Reinforcement	*Layers*	*Thickness (mm)*	*Bending stiffness (Nm²)*	Orientation of the fibre mats	Schematic	*Interface type*	
GUD + GUD	Glass UD	*4*	*1.40*		0°			UNIDIRECTIONAL
	Glass UD	*4*	*1.40*		0°			
CUD + CUD	Carbon UD	*4*	*2.07*		0°			
	Carbon UD	*4*	*2.07*		0°			
GUD + CUD	Glass UD	*7*	*2.46*	*0.93*	0°		MULTI - MATERIAL	
	Carbon UD	*4*	*2.07*	*1.01*	0°			
GUD 45	Glass UD	*8*	*2.92*		-45°/[0°]$_6$/-45°//		MULTI – DIRECTIONAL	
	Glass UD	*8*	*2.92*		+45°/[0°]$_6$/+45°			
Gf + Cf	Glass fabric	*10*	*3.39*	*1.46*	0°		MULTIMATERIAL	WOVEN FABRIC
	Carbon fabric	*9*	*2.61*	*1.50*	0°			
Gf + CUD	Glass fabric	*11*	*3.73*	*1.94*	0°			
	Carbon UD	*5*	*2.59*	*1.99*	0°			
CUD + Cf	Carbon UD	*4*	*2.07*	*1.01*	0°			
	Carbon fabric	*8*	*2.32*	*1.05*	0°			

laminates was found for any type of stacking sequence even though the interlayer thickness at the dissimilar interface increases up to 60 μm when fabrics are present at the dissimilar interlayer (S2).

$$S = EI_x = \frac{L^3 m}{4bh^3}\ \frac{bh^3}{12} = \frac{L^3 m}{48} \tag{3}$$

3. Results and discussion

3.1. Effect of interface structure on the fracture toughness of non-interleaved laminates

Prior to investigating the toughening effect of the interleaved nanofibrous veils onto the dissimilar interfaces, the delamination resistance of non-interleaved test specimens is analysed in mode I and mode II delamination tests (Fig. 3).

Overall, it is clear that the mode I IFT (G_{Ic}) of samples with a parallel oriented [UD-UD] interface is lower than for interfaces with a woven or differently oriented fibre layer. This is in agreement with previous research that showed different crack mechanisms such as crack bifurcation (branching of the cracks) and splitting (high amount of intraply damage) are present in non [UD-UD] interfaces, resulting in a higher mode I IFT initiation as well as propagation [11–15,49]. Note that for this, the ASTM standard recommends a [UD-UD] specimen design for a conservative delamination resistance value [48,50]. On the other hand, for the mode II IFT (G_{IIc}) the trend is less pronounced as the [CUD-CUD] similar laminates had a very high delamination resistance. The high GIIc for [CUD-CUD] interfaces may be due to good adhesion with the epoxy matrix and the higher specific fibre surface of carbon fibres (diameter of 7.2 μm) in comparison to glass fibres (16.5 μm) [51].

The multidirectional [GUD 45] composite has a higher mode I IFT than the [UD-UD] composites due to the formation of crack bifurcations [11,12,15]. Further, doubling of the mode I IFT is noted during propagation because of a large increase in fibre bridging and the appearance of parallel crack paths that require more energy [2,11–15,49]. For mode II on the other hand, the multidirectional glass fibre composite has a similar IFT (G_{IIc}) as the [GUD + GUD] composite because the interface fracture surface area does not vary significantly with interply angle [12].

Due to the high difference in elastic modulus between glass and carbon fibres, the stress distribution around the crack tip could alter depending on the distance to the dissimilar interface in such way that at larger distances the resulting crack will always be redirected towards the dissimilar interface. Eventually a tortuous crack development arises that induces mixed mode crack growth even though pure mode I loads are applied [9,52]. This leads to the large mode I IFT increase of the multimaterial dissimilar interface [GUD – CUD] in comparison with the similar [GUD – GUD] and [CUD – CUD] interfaces [9]. For mode II, this mechanism does not occur and the multimaterial dissimilar interface performs similar to the [CUD-CUD] interface.

High IFT values in both mode I as well as mode II IFT were obtained for multistructural and multimaterial samples containing woven fabrics at the interface because of an increased amount of parallel matrix cracks and because the transverse bundles of the woven fabric (perpendicular to the crack propagation) ensured pinning of the crack and cause it to arrest [53,54].

3.2. Effect of interface structure on nanofibre interleaved laminates

The IFT at a dissimilar interface in a composite is, on overall, substantially improved by addition of PEBA nanofibres (Fig. 4). The nanofibre toughened samples always develop a higher Strain Energy Release Rate (SERR) during the delamination test in comparison to the non-toughened reference samples under both mode I or mode II loading (Fig. 5). This is due to multiple aspects including nanofibre bridging effects and changes in the crack path. The discussion of the nanofibre

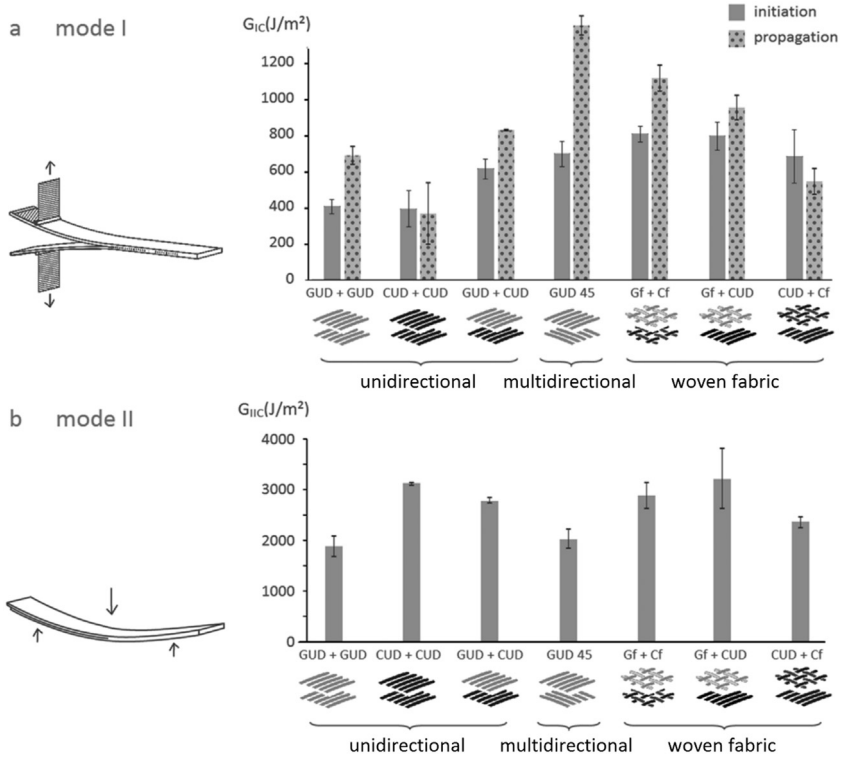

Fig. 3. The mode I (a) and mode II (b) IFT (G_{IC} and G_{IIC}) in initiation and propagation of non-interleaved composites with dissimilar interfaces including glass and carbon fibre unidirectional materials (GUD and CUD) as well as glass and carbon fibre woven fabrics (Gf and Cf).

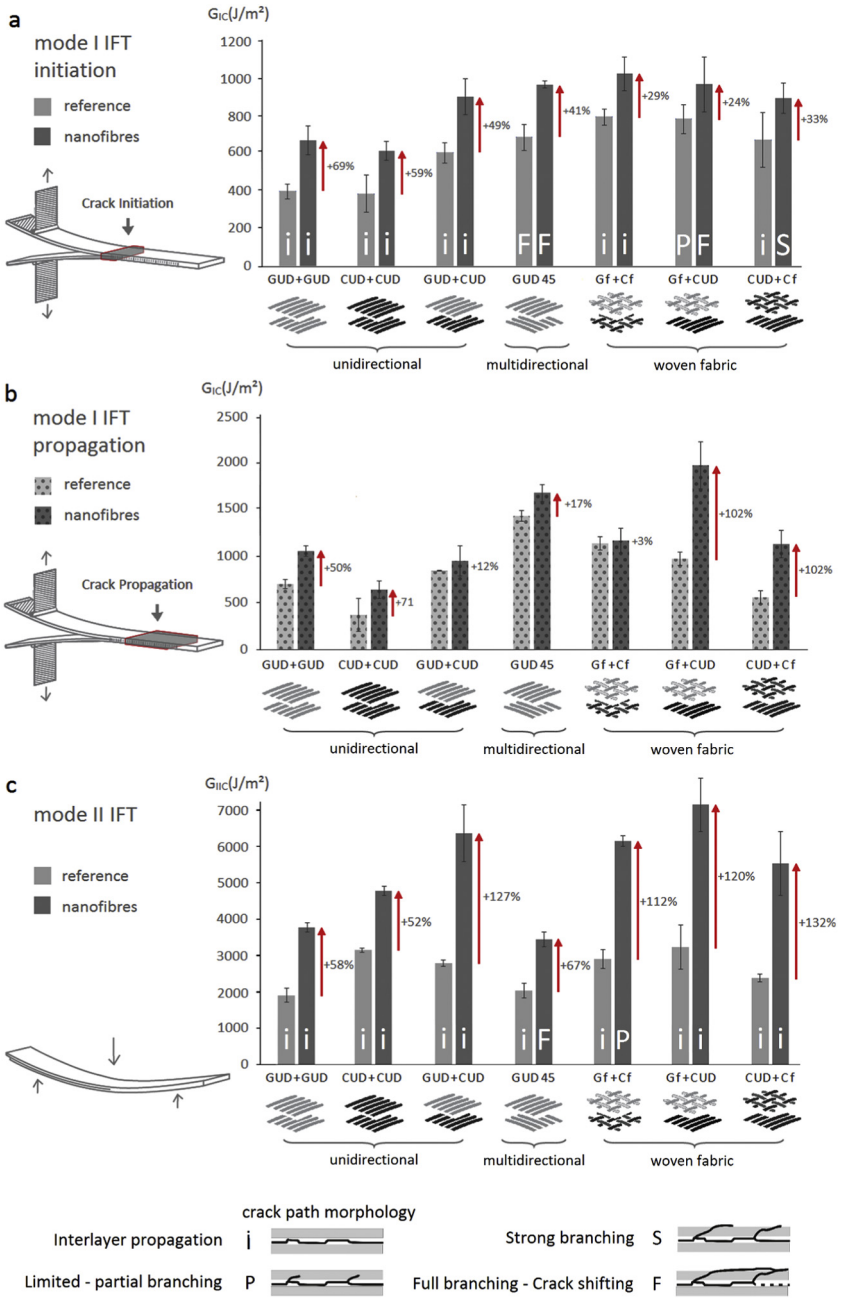

Fig. 4. All mode I and II considered dissimilar interfaces including glass (G) and carbon (C) fibre unidirectional (UD) and woven (f) fabrics benefit from nanofibre toughening. In mode I initiation (G_{IC}) ($\geq +24\%$) and mode II initiation (G_{IIC}) ($\geq +67\%$) each dissimilar interface has a vast increase in IFT that is due to the crack frequently transversing the nanofibre toughened interlayer (a, c). In mode I propagation it are the multistructural interfaces, which contain both unidirectional and woven fabrics that improve the most because of the interplay of the high increase in fracture surface area by crack bifurcations and the delamination regularly crossing the nanofibre toughened region (b).

toughening of the dissimilar interfaces is divided into three parts based on the fracture morphology.

First, the three unidirectional lay-ups will be discussed simultaneously on their nanofibre toughening performance because of their strong resemblance in fracture behaviour (Section 3.2.1). They give rise to the most prominent IFT increases in mode I initiation (Fig. 4a) because the delamination stays in the interlaminar region, which leads to a relatively smooth crack surface that allows frequent crossings through the nanofibre toughened interlaminar zone.

Second, the toughening of the GUD 45 lay-up is analysed due to its distinct fracture behaviour. It is clear that the mode I IFT of the non-toughened composite with a differently oriented fibre layer is already high in comparison to the similar case (Fig. 4a, b), which can be attributed to the formation of a rougher crack surface. When nanofibre toughening is applied at this dissimilar interfaces, a further increase in IFT is noted.

Lastly, the nanofibre toughening will be discussed of the three types of composites with woven fabrics at the dissimilar interface (-Section 3.2.3) which show high IFT increases in both mode I initiation and mode II initiation (Fig. 4a, c). Moreover, the two multistructural composites containing a [UD – f] interface provide the relatively highest increase in mode I propagation IFT of all nanofibre toughened composites (Fig. 4b) because the nanofibre toughened interlayer also forces crack bifurcations through the adjacent fabric interlayer in addition to the regular crossings through the nanofibre toughened interlayer. In addition, a detailed discussion and microscopic images of the observed

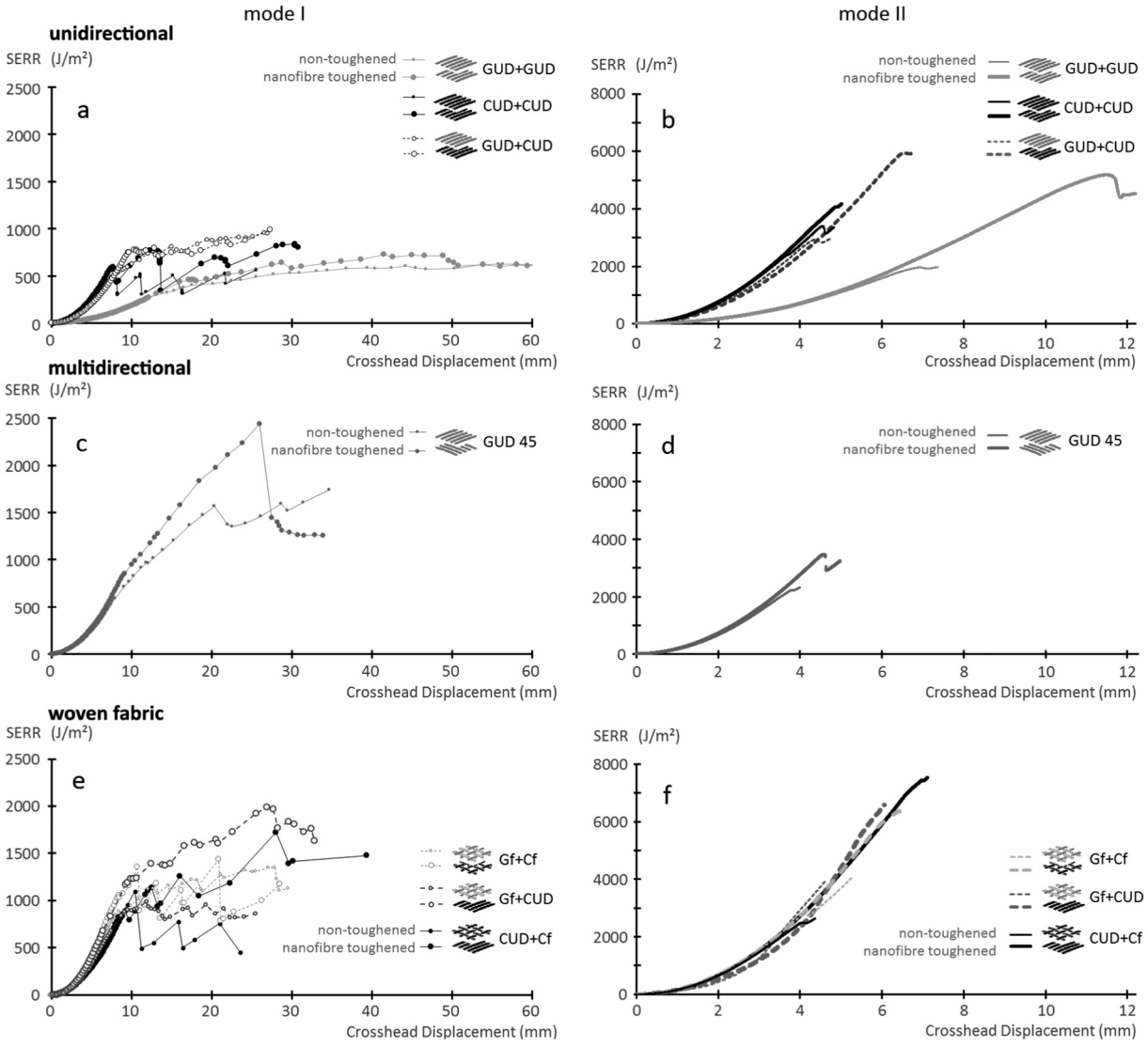

Fig. 5. For each type of interface, the development of the Strain Energy Release Rate (SERR) is shown with increasing crosshead displacement for both mode I (a,c,e) and mode II (b,d,f). Each of the nanofibre toughened composites develops a higher SERR in initiation in comparison to the non-toughened reference samples.

crack mechanisms for each type of interface is given in Supporting Information Section S4 and Section S5.

3.2.1. Nanofibre toughened composites with a unidirectional lay-up

The results in Fig. 4 show that the IFT of both mode I and II is increased by over 50% when adding PEBA nanofibre interleaves to unidirectional fibre reinforced epoxy composites with only glass or carbon fibres at the interface. This confirms our previous research on PEBA nanofibre toughening of glass fibre epoxy composites in which the fracture behaviour is discussed in detail [34]. Briefly, the fracture mechanics can be clarified when comparing lateral cross-sections of both a nanofibre toughened and a non-toughened mode I tested composite (Fig. 6a,b). The lateral cross-sections allow to clearly study the uninhibited crack development from initiation to propagation. In the case of a non-toughened unidirectional composite, the crack propagates relatively smoothly within the resin rich interlayer (Fig. 6a). In comparison, for nanofibre toughened specimens, the crack stays within the interlayer, but now frequently passes through the nanofibre toughened region (Fig. 6b,c). During these crossings of the crack, many tough PEBA nanofibres were plastically deformed and broken (Fig. 6d), which ultimately leads to high increases in IFT. The delamination and toughening mechanism of the multimaterial [GUD-CUD] composite thus remains comparable to that of similar unidirectional composites and is further discussed in detail in Supporting Information Section S3 and Section S4.

3.2.2. Nanofibre toughened multidirectional interface

The delamination experiments previously shown in Fig. 3 show that the non-toughened reference sample of the multidirectional [GUD 45] composite already has a high fracture toughness, certainly compared to unidirectional mode I reference samples. Nanofibres are even able to further increase the IFT by 41% in mode I (initiation) and 67% in mode II (initiation) (Fig. 4a, c, multidirectional).

Fig. 7a,b shows the lateral cross section in the direction of propagation of a mode I tested [GUD 45] composite. Both the delaminations of the non-toughened reference sample and the nanotoughened sample create side-branches, but in case of the nanotoughened sample the main delamination eventually leaves the dissimilar interface and continues propagating at a neighbouring interface after several mm of crack growth. This is possibly because the delamination was obstructed by the nanofibre-toughened region considering too much energy is needed to propagate through this zone. This was also confirmed by limited toughness increase in mode I propagation (Fig. 4b,

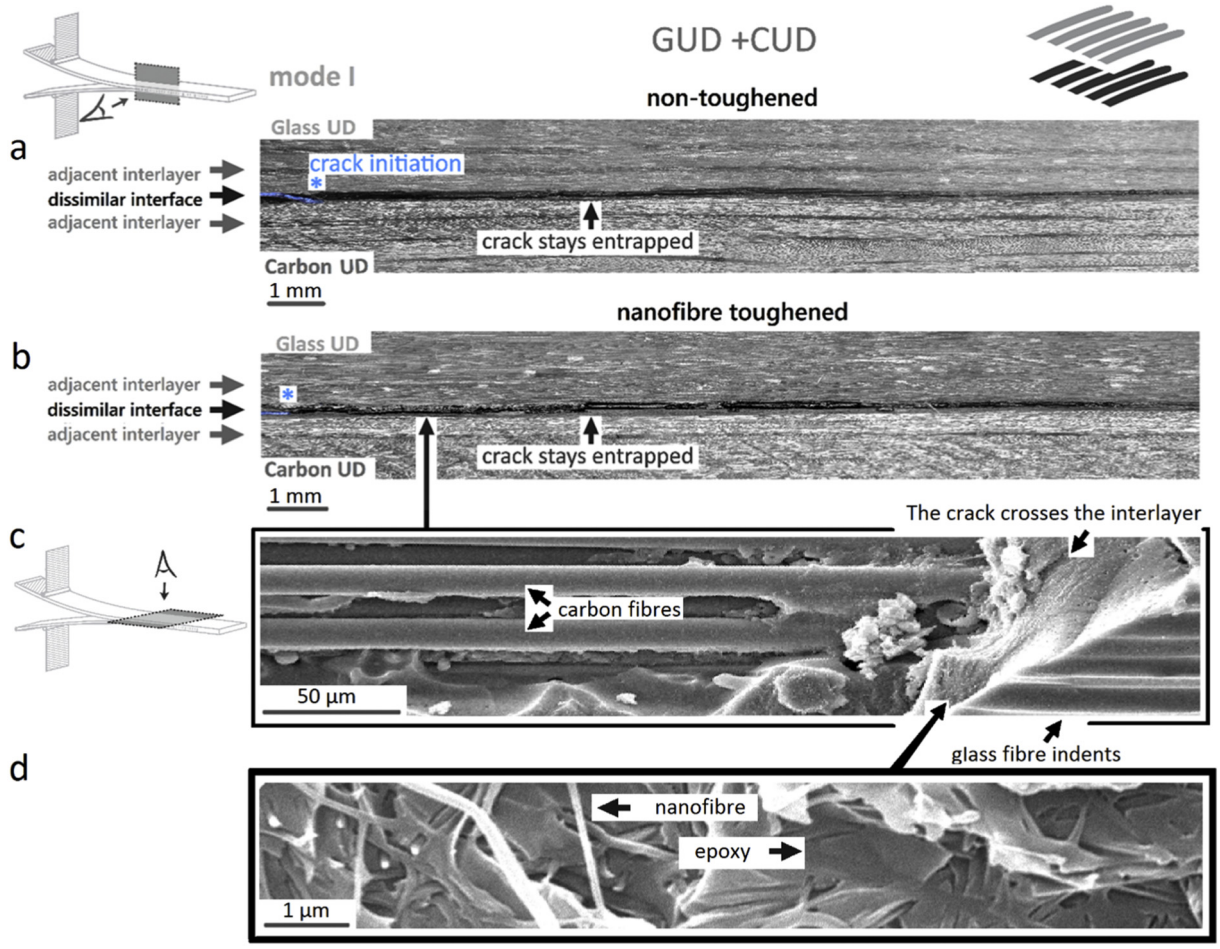

Fig. 6. The lateral cross section of a mode I tested unidirectional multimaterial composite [GUD-CUD] without nanofibres (a) shows that the crack propagates evenly within the unidirectional interface. In case of a nanofibre toughened composite (b), the crack alternates between both sides of the interlayer and repeatedly crosses the nanofibre toughened interlaminar region (c) that results in plastic deformations of the nanofibres (d) and a high IFT increase. A similar fracture development is noted for the equivalent similar GFRP (S3) and CFRP.

multidirectional). At first, the nanofibres influence the delamination, but this effect is diminished during crack growth as the delamination moves towards a neighbouring interface. Note that the calculation of the propagation fracture toughness used here does not consider changes in loading mode or delamination area caused by delaminations moving towards other interfaces, and is thus rather a measure for energy absorption during the delamination experiment than an intrinsic material parameter.

This effect is also present for mode II loaded samples where the crack remains in the central interlayer for non-toughened specimens, but immediately moves towards the neighbouring interface for nanofibre toughened specimens (Fig. 7c, d). This results in a vast increase in the measured IFT (Fig. 4c) and demonstrates that the crack needs less energy to propagate through the reinforcement layer in comparison to the nanofibre toughened interlayer. Note that the obtained G_{II} value for the nanofibre toughened specimens might not be correctly calculated, and thus differ slightly, as the deviation from the main delamination results in an asymmetrical specimen and normally a symmetrical specimen is assumed for Eq. (2). Additionally, there is still some torsion coupling possible for the tested samples because both arms of the samples have off-axis fibre orientation of +45° and − 45° for the bottom and the top part.

3.2.3. Nanofibre toughened composites with a woven fabric at the dissimilar interface

The fracture behaviour of different nanofibre toughened composites with a woven fabric at the dissimilar interface show strong similarities to each other due to the interaction of the crack path with the waviness of the woven fabrics. Three types of these interfaces are discussed, namely [Gf + Cf], [CUD + Cf] and [CUD + Gf]. Separate optical microscopy cross sections of mode I and II tested samples of each of the three interfaces are added in Section S4 and Section S5.

The non-toughened composites already have a high fracture toughness because of the woven architecture of the reinforcement fabrics, yet they are still greatly improved by addition of nanofibres (Fig. 4, woven fabric). The woven structures make the delamination path more irregular as can be seen for the [CUD + Cf] interface as an example in Fig. 8a–d, which results in a larger crack surface and thus more absorbed energy.

The two interfaces that also contain UD reinforcement ([CUD + Cf] and [CUD + Gf]) at the interface have a very high increase in propagation toughness of over 100% on the non-toughened specimens. This is an indication that the interaction between the crack path and the nanofibre toughened interface becomes better upon mode I crack propagation. The difference in reinforcement structure makes the delamination crack path more irregular (Fig. 8). When considering the mode I samples, the main delamination follows the relatively smooth UD fibre reinforcement with short side branches diverging into the woven structure of the fabric. In the case of the reference sample, these side branches always return to the main delamination (Fig. 8a), while the delamination growth of the nanofibre-toughened sample is similar, but has side-branches propagating completely through the neighbouring interface in parallel to the main delamination over the entire crack length (Fig. 8b). Hence, the crack surface of the nanofibre-

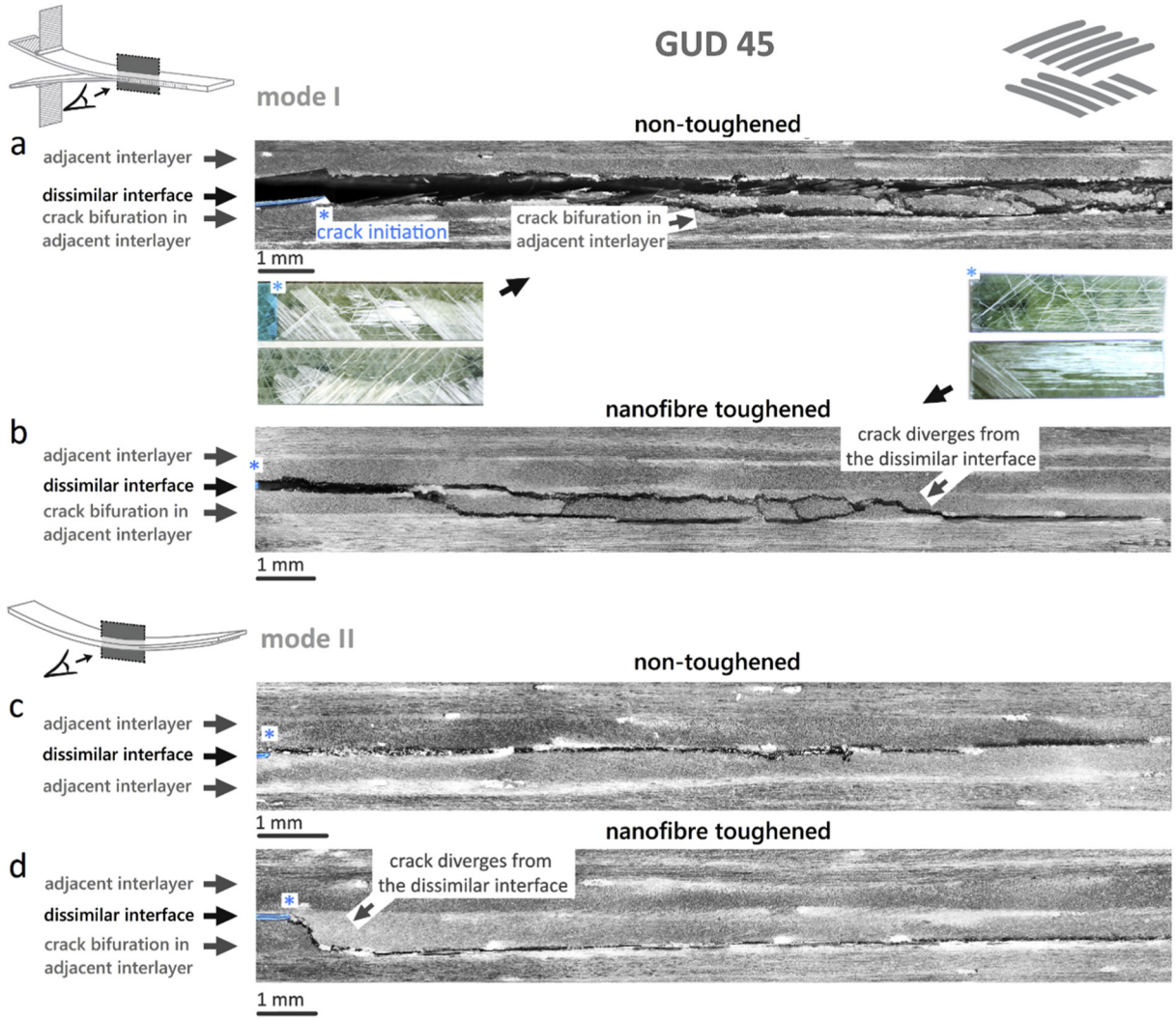

Fig. 7. The lateral cross sections along the direction of propagation (from left to right) of delaminated mode I and mode II composites without nanofibres (a,c) and with nanofibres (b,d) are shown and give insights on the effects of nanofibre toughening on the crack path. The top-view of the optical microscopy insert of a non-toughened reference sample clearly shows an asymmetric fracture pattern indicating oblique crack growth due to torsion coupling. In the nanofibre toughened composites, the crack completely shifts towards the neighbouring interlayer during propagation, for both mode I and mode II, indicating the crack tries to avoid the highly toughened (dissimilar) interlayer.

toughened sample is bigger (almost doubled as there are two delaminations), which together with the nanofibre bridging effect explains the large increase in IFT in mode I propagation compared to mode I initiation. In the case of the mode I tested [Gf – Cf] specimens (Section S4), the crack stays within the interlaminar region without deviating into the neighbouring interlayer for both reference and nanofibre toughened specimens. The added IFT here is thus attributed to the interaction between the crack path and the toughened interlayer solely. Because the crack mainly propagates on the glass fabric reinforcement side of the interface, the mode I [Gf + CUD] interface results in similar values for the mode I IFT tested [Gf + Cf] sample. In both cases, the delamination propagates mainly through the glass fibre reinforcement, which implies that the neighbouring carbon reinforcement, be it unidirectional or fabric, has little to no influence on the crack path behaviour. This could be because the glass fibre-epoxy adhesion is worse than the carbon fibre-epoxy adhesion.

The crack path of mode II tested specimens is similar for all three specimens for both non-toughened and toughened laminates. It follows the warp yarns without substantial bifurcations through the laminate except in the case of [Gf + Cf] where occasional bifurcations occurred, but were always redirected back by the surrounding part of the crack that does remain within the dissimilar interface (S4).

4. Conclusion

We can conclude that the nanofibre toughening is beneficial in practical applications where dissimilar interfaces form a damage-prone boundary between composite plies having different structural or mechanical properties. For all of the considered dissimilar interfaces an overall increase is noted of 30–50% in mode I and 70–130% in mode II initiation IFT. This is due to multiple aspects including nanofibre bridging effects, the inherent toughness and plastic deformation of the nanofibres and the frequent crossings of the crack path through the nanofibre toughened interlaminar zone. Besides the direct effects of the nanofibre toughening itself, we have also shown that augmented occurrence of crack bifurcations towards adjacent non-toughened interlayers is an important factor for the improved IFT, which also explains why the increase in mode I propagation IFT (100%) is most substantial for multistructural composites.. These bifurcations were likely induced by the inherent higher toughness of the interlayer at the dissimilar interface. Thus, this novel insight suggests that in the majority of cases the dissimilar interface is toughened to such a degree that the adjacent interlayers might need to be toughened to achieve optimum results. Though, design-wise this may exceed what is necessary as it is much simpler to have just one nanofibrous layer at the specific damage-

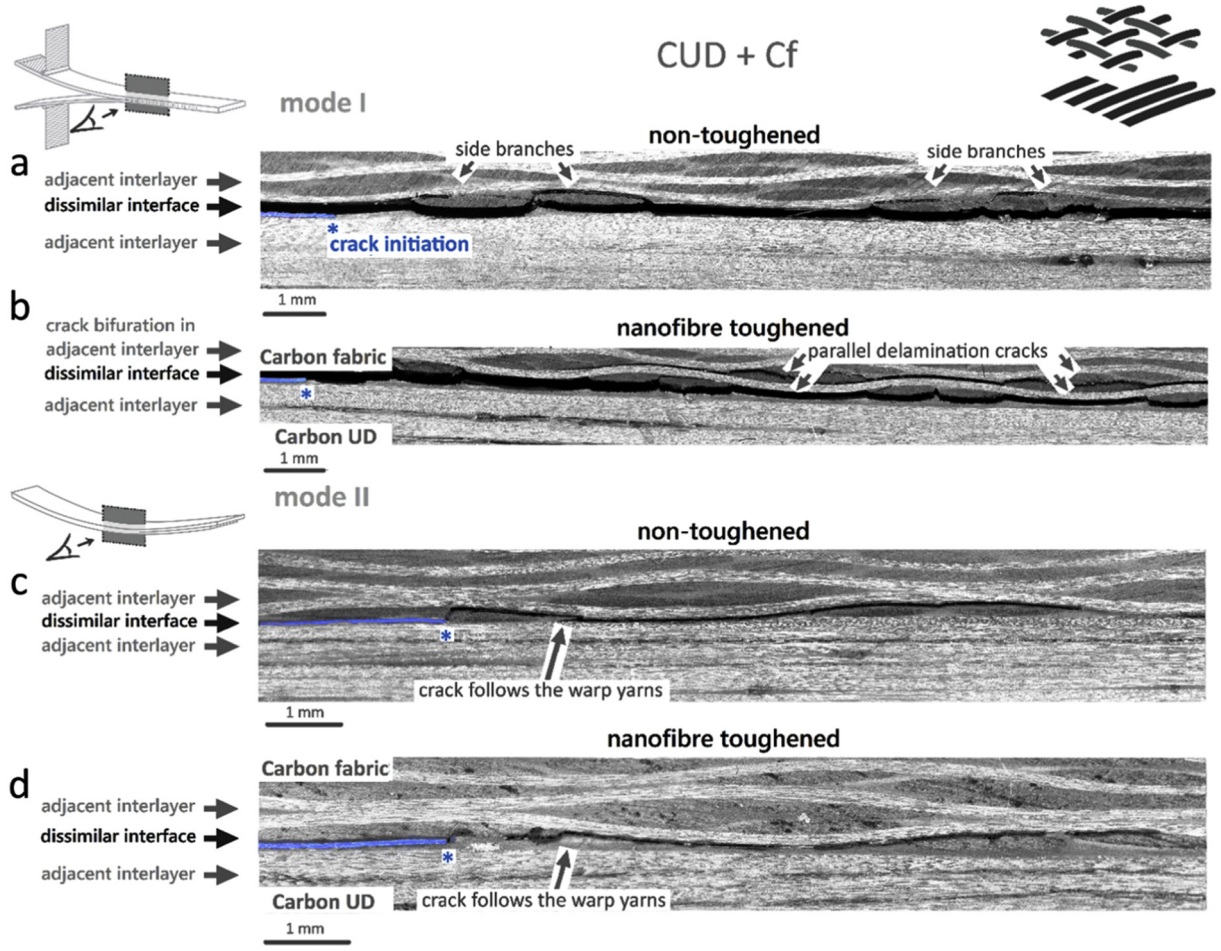

Fig. 8. When comparing the mode I propagation of non-toughened (a) and nanofiber toughened (b) samples, the high increase in mode I propagation IFT (Fig. 4b) of the composites that still have unidirectional fibres at the interface can be explained. The nanofibre toughened composite shows many crack bifurcations and the formation of a second major interlaminar crack propagating in parallel at the adjacent interlayer. In contrast, the [Gf + Cf] interface (supplementary information Fig. S4.2) does not show any significant crack bifurcations and thus the IFT in mode I propagation does not drastically increase. The high mode II IFT (G_{IIC}) increases are due to the crack propagating through the nanofibre toughened interlayer thereby regularly crossing the nanofibres (b,d).

prone dissimilar interface instead of throughout the laminate. The absence of any resin viscosity increase in addition to the ease of applying nanofibre toughening could possibly open up opportunities towards industrial composite toughening near dissimilar interfaces.

Data availability

The raw data required to reproduce these findings cannot be shared at this time as the data also forms part of an ongoing study. The processed data required to reproduce these findings cannot be shared at this time as the data also forms part of an ongoing study.

Declaration of Competing Interest

The authors declare that they have no known competing financial interests or personal relationships that could have appeared to influence the work reported in this paper.

Acknowledgements

Lode Daelemans acknowledges support from Research Foundation – Flanders (FWO) (grant number FWO.3E0.2019.0043.01). T.M., L.D., W.V.P. and K.D.C. gratefully acknowledge financial support from Ghent University (BOF 13/24J/020 and BOF.PDO.2015.0028.01).

Appendix A. Supplementary data

Supplementary data to this article can be found online at https://doi.org/10.1016/j.matdes.2020.109050.

References

[1] L. Belgacem, D. Ouinas, J. Aurelio, V. Olay, A. Argüelles, Experimental investigation of notch e ff ect and ply number on mechanical behavior of interply hybrid laminates (glass / carbon / epoxy), Compos. Part B 145 (2018) 189–196, https://doi.org/10.1016/j.compositesb.2018.03.026.
[2] M. Nikbakht, H. Hosseini Toudeshky, B. Mohammadi, Experimental study on the effect of interface fiber orientation and utilized delamination initiation techniques on fracture toughness of glass/epoxy composite laminates, J. Reinf. Plast. Compos. 35 (2016) 1722–1733.
[3] J. Zhang, K. Chaisombat, S. He, C.H. Wang, Hybrid composite laminates reinforced with glass / carbon woven fabrics for lightweight load bearing structures, Mater. Des. 36 (2012) 75–80, https://doi.org/10.1016/j.matdes.2011.11.006.
[4] Y. Swolfs, Perspective for Fibre-Hybrid Composites in Wind energy application, Materials (Basel) 10 (2017) https://doi.org/10.3390/ma10111281.
[5] C. Dong, I.J. Davies, Flexural and tensile strengths of unidirectional hybrid epoxy composites reinforced by S-2 glass and T700S carbon fibres, Mater. Des. 54 (2014) 955–966, https://doi.org/10.1016/j.matdes.2013.08.087.
[6] H. Liu, B.G. Falzon, W. Tan, Composites : Part A Predicting the Compression-After-Impact (CAI) strength of damage-tolerant hybrid unidirectional/woven carbon-fibre reinforced composite laminates, Compos. Part A 105 (2018) 189–202, https://doi.org/10.1016/j.compositesa.2017.11.021.

[7] H. Liu, B.G. Falzon, W. Tan, Experimental and numerical studies on the impact response of damage- tolerant hybrid unidirectional / woven carbon- fi bre reinforced composite laminates, Compos. Part B 136 (2018) 101–118, https://doi.org/10.1016/j.compositesb.2017.10.016.

[8] M.J. Mathews, S.R. Swanson, A numerical approach to separate the modes of fracture in interface crack propagation, J. Compos. Mater 39 (2004) https://doi.org/10.1177/0021998305046449.

[9] S. Hwang, B. Shen, Opening-Mode Interlaminar Fracture Toughness of Interply Hybrid Composite Materials, 59, 1999.

[10] S. Hwang, C. Huang, Sliding Mode Interlaminar Fracture Toughness of Interply Hybrid Composite Materials, 1998.

[11] N.S. Choi, A.J. Kinloch, J.G. Williams, Delamination fracture of multidirectional carbon-fiber/epoxy composites under mode I, mode II and mixed-mode I/II loading, J. Compos. Mater. 33 (1998).

[12] Y.B. Shi, D. Hull, Mode II fracture of +Θ/−Θ angled laminate interfaces, Compos. Sci. Technol. 47 (1993) 173–184, https://doi.org/10.1016/0266-3538(93)90045-I.

[13] A. Desai, C.M. Sharanaprabhu, S.K. Kudari, Experimental investigation on the effects of fiber orientation on translaminar fracture toughness for glass-epoxy composite under mixed Mode I/II load, AIP Conf. Proc. 2057 (2019)https://doi.org/10.1063/1.5085581.

[14] A.B. Pereira, A.B. de Morais, Mode I interlaminar fracture of carbon/epoxy multidirectional laminates, Compos. Sci. Technol. 64 (2004) 2261–2270, https://doi.org/10.1016/j.compscitech.2004.03.001.

[15] J.P. Lucas, Delamination fracture: effect of fiber orientation on fracture of a continuous fiber composite laminate, Eng. Fract. Mech. 42 (1992) 543–561.

[16] Reprinted from Wind Energy, 21, R.W. Martin, A. Sabato, A. Schoenberg, R.H. Giles, C. Niezrecki, Comparison of nondestructive testing techniques for the inspection of wind turbine blades' spar caps, 980–996, Copyright (2020), with permission from John Wil, (2018).

[17] Reprinted from Materials & Design, 60, E. Sevkat, H. Turner, M. Halidun Kelestemur, S. Dogan, Effect of torsional strain-rate and lay-up sequences on the performance of hybrid composite shafts, Copyright (2020), with permission from Elsevier, (2014).

[18] Reprinted from Materials & Design, 51, E. Sevkat, H. Turner, Residual torsional properties of composite shafts subjected to impact loadings, 956–967, Copyright (2020), with permission from Elsevier, (2013).

[19] Reprinted from Materials & Design, 183, W. Fan, W. Dang, T. Liu, J. Li, L. Xue, L. Yuan, J. Dong, Fatigue behavior of the 3D orhogonal carbon/glass fibers hybrid composite under three-point bending load, 1–9, Copyright (2020), with permission from Elsevie, (2019).

[20] Reprinted from Materials & Design, 36, J. Zhang, K. Chaisombat, S. He, C.H. Wang, Hybrid compositelaminates reinforced with glass / carbon woven fabrics for lightweight load bearing structures, 75–80, Copyright (2020), with permission from Elsevier, (2012).

[21] Reprinted from Materials & Design, 31, H.S.S. Aljibori, W.P. Chong, T.M.I. Mahlia, W.T. Chong, P. Edi, H. Al-qrimli, I. Anjum, R. Zahari, Load-displacement behavior of glass fiber/epoxy composite plates with circular cut-outs subjected to compressive load, (2010).

[22] Reprinted from Materials & Design, 31, H. Ghasemnejad, H. Hadavinia, A. Aboutorabi, Effect of delamination failure in crashworthiness analysis of hybrid composite box structures, 1105–1116, Copyright (2020), with permission from Elsevier, (2010).

[23] J.S. Kim, D.H. Reneker, Mechanical properties of composites using ultrafine electrospun fibers, Polym. Compos. 20 (1999) 124–131, https://doi.org/10.1002/pc.10340.

[24] K. Bilge, E. Ozden-Yenigun, E. Simsek, Y.Z. Menceloglu, M. Papila, Structural composites hybridized with epoxy compatible polymer/MWCNT nanofibrous interlayers, Compos. Sci. Technol. 72 (2012) 1639–1645, https://doi.org/10.1016/j.compscitech.2012.07.005.

[25] K. Bilge, Y. Yorulmaz, F. Javanshour, A. Ürkmez, B. Yılmaz, E. Şimşek, M. Papila, Synergistic role of in-situ crosslinkable electrospun nanofiber/epoxy nanocomposite interlayers for superior laminated composites, Compos. Sci. Technol. 151 (2017) 310–316, https://doi.org/10.1016/j.compscitech.2017.08.029.

[26] L. Daelemans, S. Van Der Heijden, I. De Baere, H. Rahier, W. Van Paepegem, K. De Clerck, Damage-resistant composites using electrospun Nanofibers: a multiscale analysis of the toughening mechanisms, ACS Appl. Mater. Interfaces 8 (2016) 11806–11818, https://doi.org/10.1021/acsami.6b02247.

[27] R. Palazzetti, A. Zucchelli, Electrospun nanofibers as reinforcement for composite laminates materials – a review, Compos. Struct. 182 (2017) 711–727, https://doi.org/10.1016/j.compstruct.2017.09.021.

[28] Y.A. Dzenis, D.H. Reneker, Delamination Resistant Composites Prepared by Small Diameter Fiber Reinforcement at Ply Interfaces, United States Patent 6265333 2001.

[29] L. Daelemans, N. Kizildag, W. Van Paepegem, R.D. Dagmar, K. De Clerck, Interdiffusing core-shell nanofiber interleaved composites for excellent Mode I and Mode II delamination resistance, Compos. Sci. Technol. 175 (2019) 143–150, https://doi.org/10.1016/j.compscitech.2019.03.019.

[30] F. Sarasini, J. Tirillò, I. Bavasso, M. Paola, F. Sbardella, L. Lampani, G. Cicala, Effect of electrospun nanofibres and MWCNTs on the low velocity impact response of carbon fibre laminates, 234, 2020, pp. 1–18, https://doi.org/10.1016/j.compstruct.2019.111776.

[31] T. Review, A review on electrospinning design and nanofibre assemblies, 2006 https://doi.org/10.1088/0957-4484/17/14/R01.

[32] E. Tech, Electrospinning Mass production machine providors, http://electrospintech.com/massproductionmachine.html#.XxBq8v4zaHt 2017.

[33] G.W. Beckermann, K.L. Pickering, Mode i and Mode II interlaminar fracture toughness of composite laminates interleaved with electrospun nanofibre veils, Compos. Part A Appl. Sci. Manuf. 72 (2015) 11–21, https://doi.org/10.1016/j.compositesa.2015.01.028.

[34] T. Meireman, L. Daelemans, S. Rijckaert, H. Rahier, W. Van Paepegem, K. De Clerck, Delamination resistant composites by interleaving bio-based long-chain polyamide nanofibers through optimal control of fiber diameter and fiber morphology, Compos. Sci. Technol. 193 (2020) 108126, https://doi.org/10.1016/j.compscitech.2020.108126.

[35] E. Özden-Yenigün, K. Bilge, E. Sünbüloğlu, E. Bozdağ, M. Papila, High strain rate response of nanofiber interlayered structural composites, Compos. Struct. (2017) 47–55, https://doi.org/10.1016/j.compstruct.2017.02.007.

[36] L. Daelemans, S. van der Heijden, I. De Baere, H. Rahier, W. Van Paepegem, K. De Clerck, Nanofibre bridging as a toughening mechanism in carbon/epoxy composite laminates interleaved with electrospun polyamide nanofibrous veils, Compos. Sci. Technol. 117 (2015) 244–256, https://doi.org/10.1016/j.compscitech.2015.06.021.

[37] S. Hamer, H. Leibovich, A. Green, R. Intrater, R. Avrahami, E. Zussman, A. Siegmann, D. Sherman, Mode i interlaminar fracture toughness of Nylon 66 nanofibrilmat interleaved carbon/epoxy laminates, Polym. Compos. 32 (2011) 1781–1789, https://doi.org/10.1002/pc.21210.

[38] J. Zhang, T. Yang, T. Lin, C.H. Wang, Phase morphology of nanofibre interlayers: critical factor for toughening carbon/epoxy composites, Compos. Sci. Technol. 72 (2012) 256–262, https://doi.org/10.1016/j.compscitech.2011.11.010.

[39] B. Beylergİl, M. Tanoğlu, E. Aktaş, Modification of carbon fibre/epoxy composites by polyvinyl alcohol (PVA) based electrospun nanofibres, 2016 69–76, https://doi.org/10.1177/096369351602500303.

[40] H. Saghafi, T. Brugo, G. Minak, A. Zucchelli, Composites : Part B The effect of PVDF nanofibers on mode-I fracture toughness of composite materials, 72, 2015 213–216, https://doi.org/10.1016/j.compositesb.2014.12.015.

[41] S. van der Heijden, L. Daelemans, K. De Bruycker, R. Simal, I. De Baere, W. Van Paepegem, H. Rahier, K. De Clerck, Novel composite materials with tunable delamination resistance using functionalizable electrospun SBS fibers, Compos. Struct. 159 (2017) 12–20, https://doi.org/10.1016/j.compstruct.2016.09.057.

[42] B. Mahmoud, L. Manseri, A. Rogani, P. Navarro, S. Marguet, J.F. Ferrero, I. Tawk, Experimental and numerical study of the damage mechanisms in hybrid unidirectional/woven composites under impact loading, Compos. Struct. 209 (2019) 606–615, https://doi.org/10.1016/j.compstruct.2018.10.098.

[43] M. Yuan He, A.G. Evans, J.W. Hutchinson, Crack deflection at an interface between dissimilar elastic materials: role of residual stresses, Int. J. Solids Struct. 31 (1994) 3443–3455.

[44] H. Ming-Yuuan, J.W. Hutchinson, Crack deflection at an interface between dissimilar elastic materials, Int. J. Solids Struct. 25 (1989) 1053–1067.

[45] D. Leguillon, C. Lacroix, E. Martin, Crack deflection by an interface - asymptotics of the residual thermal stresses, Int. J. Solids Struct. 38 (2001) 7423–7445.

[46] M.D. Abràmoff, P.J. Magalhães, S.J. Ram, Image processing with imageJ, Biophoton. Int. 11 (2004) 36–41, https://doi.org/10.1117/1.3589100.

[47] A. Arrese, N. Carbajal, G. Vargas, F. Mujika, A new method for determining mode II R-curve by the end-notched flexure test beam theory including bending rotations, Eng. Fract. Mech. 77 (2010) 51–70, https://doi.org/10.1016/j.engfracmech.2009.09.008.

[48] ASTM Standard D5528-13, Standard Test Method for Mode I Interlaminar Fracture Toughness of Unidirectional Fiber-Reinforced Polymer Matrix Composites, ASTM International, West Conshohocken, PA, 2013 https://doi.org/10.1520/D5528-13.

[49] A.C. Orifici, P. Wongwichit, N. Wiwatanawongsa, Embedded flaws for crack path control in composite laminates, Compos. Part A Appl. Sci. Manuf. 66 (2014) 218–226, https://doi.org/10.1016/j.compositesa.2014.08.012.

[50] ASTM Standard D7905 / D7905M-14, Standard Test Method for Determination of the Mode II Interlaminar Fracture Toughness of Unidirectional Fiber-Reinforced Polymer Matrix Composites, 2014 https://doi.org/10.1520/D7905_D7905M-14.

[51] D. Chen, G. Sun, M. Meng, X. Jin, Q. Li, Flexural performance and cost efficiency of carbon/basalt/glass hybrid FRP composite laminates, Thin-Walled Struct. 142 (2019) 516–531, https://doi.org/10.1016/j.tws.2019.03.056.

[52] M.L. Williams, The stresses around a fault or crack in dissimilar media, Bull. Seismol. Soc. Am. 49 (1959) 199–204.

[53] T. Ogasawara, A. Yoshimura, T. Ishikawa, R. Takahashi, Interlaminar fracture toughness of 5 harness satin woven fabric carbon fiber / epoxy, Composites 21 (2012) 45–56, https://doi.org/10.1163/156855112X626219.

[54] J.R.S. De Aja, F.M. De Escalera, P. Cruz, A. Ortega, P. Maimí, E.V. Gonz, Translaminar fracture toughness of interply hybrid laminates under tensile and compressive loads, 143, 2017 https://doi.org/10.1016/j.compscitech.2017.02.029.